

Measurement of the Helicity Difference in Double - Pion  
Photoproduction using the CLAS Spectrometer at  
Jefferson Laboratory

Prospectus of Dissertation

Sungkyun Park

Department of Physics, Florida State University

November 18, 2008

Major professor: Volker Crede  
committee member: Paul Eugenio  
committee member: Simon Capstick  
committee member: Todd Adams  
committee member: Tomasz Plewa

# Abstract

Jefferson Laboratory (JLAB) has experiments to find the excited states of baryons. However, most of these experiments at JLAB have used unpolarized targets. Experiments using polarized targets are needed to find observables related to the target. The CLAS frozen spin target (FROST) experiment satisfies the conditions toward a “complete” experiment. In this prospectus of dissertation, the motivation and methods for calculating the helicity difference,  $P_z^\odot$ , for the reaction  $\gamma p \rightarrow p\pi^+\pi^-$  will be discussed. I participated in this experiment from the stage of the data taking. I will discuss my efforts to advance the FROST experiment through my duties in reconstructing the FROST data, managing the monitoring web, and calibrating the drift chamber (DC).

# 1 Introduction

The nucleus of an atom consists of protons and neutrons called baryons. The baryon is further composed of subatomic fundamental particles known as quarks, bound by the strong interaction<sup>1</sup>. Quantum Chromodynamics (QCD) is the theory of how quarks and gluons<sup>2</sup> interact with themselves and each other.

The mass of the proton is nearly 50 times greater than the bare masses of its constituent quarks. The force between quarks does not diminish as they are separated so quarks cannot be separated from the baryon. The description of masses, widths, and other decay properties of these baryon states requires QCD-based models of the baryon structure. The most useful models are based on three constituent quark degrees of freedom (constituent quark models, CQMs). In addition to a linear confinement potential, CQMs adopt one-gluon exchange [1], Goldstone boson exchange [2], or instanton-induced interactions [3] as the short-range interaction between quarks.

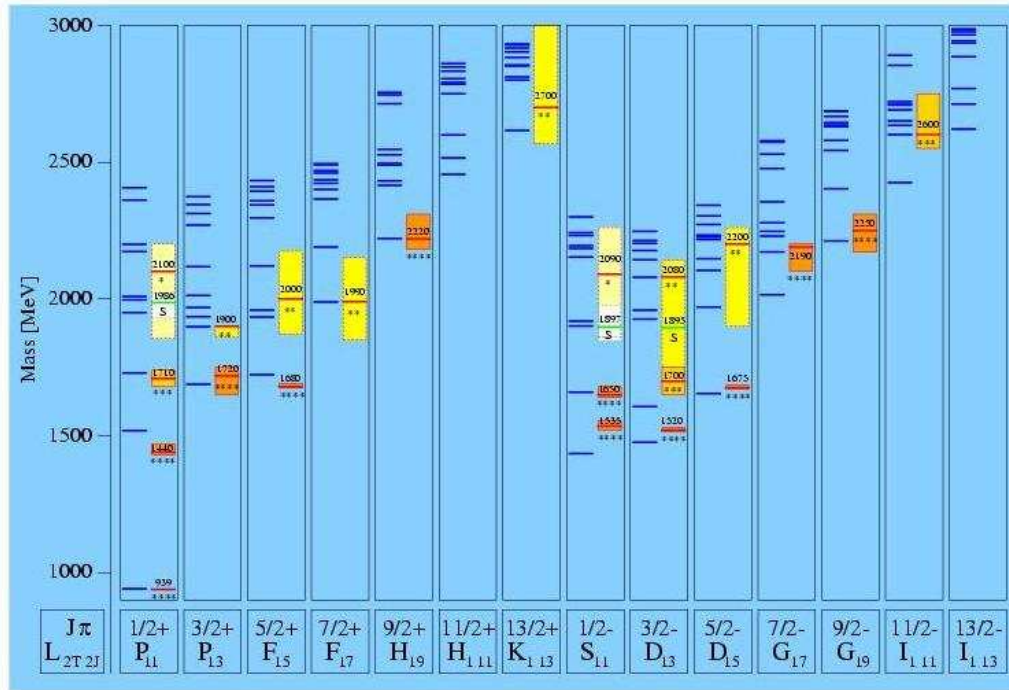


Figure 1:  $N^*$  resonances using instantons as short-range interaction. The left side of each column shows model predictions based on instanton-induced interactions [3], whereas the corresponding right side illustrates experimental findings. The number of \*'s indicates the ranking of the state according to the PDG, i.e. a four-star state being a well established resonance.

Figure 1 describes the predictions of the instanton-based model and the experimental findings of  $N^*$  resonances. The excited states suggested by models do not match accurately the states measured by the experiment,

<sup>1</sup>The strong interaction is one of the four fundamental interactions, along with gravitation, the electromagnetic force and the weak interaction. This force is mediated by gluons and holds the proton together.

<sup>2</sup>Gluons are elementary particles that cause quarks to interact

excluding  $P_{11}(939)$  called the nucleon. Above 2 GeV models also predict more states than have been seen in the data. These missing states denote additional states predicted by models which do not match the states found by experiments and they are distributed mainly in the range above  $\sim 2000$  MeV/ $c^2$ . Probably, more accurate predictions from lattice-QCD calculations, derived from a fundamental quantum field theory, will be available in the future. In this situation, the CQMs may become obsolete. Nevertheless, they give us a good idea of determining which physics regions should be explored and where exciting physics can be expected.

Constituent quark models are very useful to describe the masses of low-lying states. At higher energies, however, many of the predicted excited baryon states do not seem to be realized in nature. The following reasons might account for this phenomenon:

- Most experiments have been  $N\pi$  elastic scattering experiments. If the unobserved resonances do not couple to  $N\pi$ , they would not have been found in this process.
- Photoproduction data accumulated in recent years mainly cover masses up to 1800 MeV/ $c^2$ . The additional resonances are predicted to exist in the mass region at and above this value.
- Most channels explored until now include one meson in the final state. However, many high-mass resonances do not decay directly into the ground state via single-meson emission but via a sequential decay chain.

The excited states of the nucleon, which we are interested in, do not exist as cleanly separated spectral lines. In real measurements, the excited states are found as broadly overlapping resonances which may decay into a multitude of final states involving mesons and baryons. Usually, these overlapping resonances display themselves more clearly through interference with dominant amplitudes. We can isolate single resonances from these other interference terms by determining the polarization observables.

## 2 Motivation for this work

The investigation of 3-body final states can be the key for discovering properties of high mass missing states because they account for most of the cross section above  $W \approx 1.7$  GeV. These missing states are predicted to decay into higher excited intermediate states rather than a ground-state nucleon and a meson. High-mass states which yield total widths of at least 150 MeV, have wider partial widths than 2-body final states like  $N\pi$ . Thus the remaining decay strength must lie in reactions with higher thresholds.

The investigation of double-pion photoproduction is one of the key experiments in the search for missing states. Quark models predict  $\gamma N \rightarrow N^* \rightarrow \Delta\pi \rightarrow N\pi^+\pi^-$  and  $\gamma N \rightarrow N^* \rightarrow N\rho \rightarrow N\pi^+\pi^-$  as dominant resonant decay modes leading to  $\gamma p \rightarrow p\pi^+\pi^-$ . However, these modes are difficult to detect since detectors with

a large angular acceptance are needed and large non-resonant background contributes. It is very effective to use data taken with the CLAS spectrometer at JLab because CLAS is a large-acceptance spectrometer optimized for the detection of charged particles and this experiment has the newly developed frozen-spin target (FROST) in order to measure the important polarization observables for this reaction.

### 3 FROST Experiment

#### 3.1 Experimental Setup

##### 3.1.1 CEBAF Large Acceptance Spectrometer (CLAS)

The Continuous Electron Beam Accelerator Facility (CEBAF) at Jefferson Laboratory can deliver a continuous electron beam up to  $\sim 6$  GeV to three experimental areas (Halls A, B, and C). The CLAS spectrometer housed in Hall B is based on six superconducting coils producing a toroidal magnetic field. The coils divide CLAS into six sectors as shown in Figure 2.

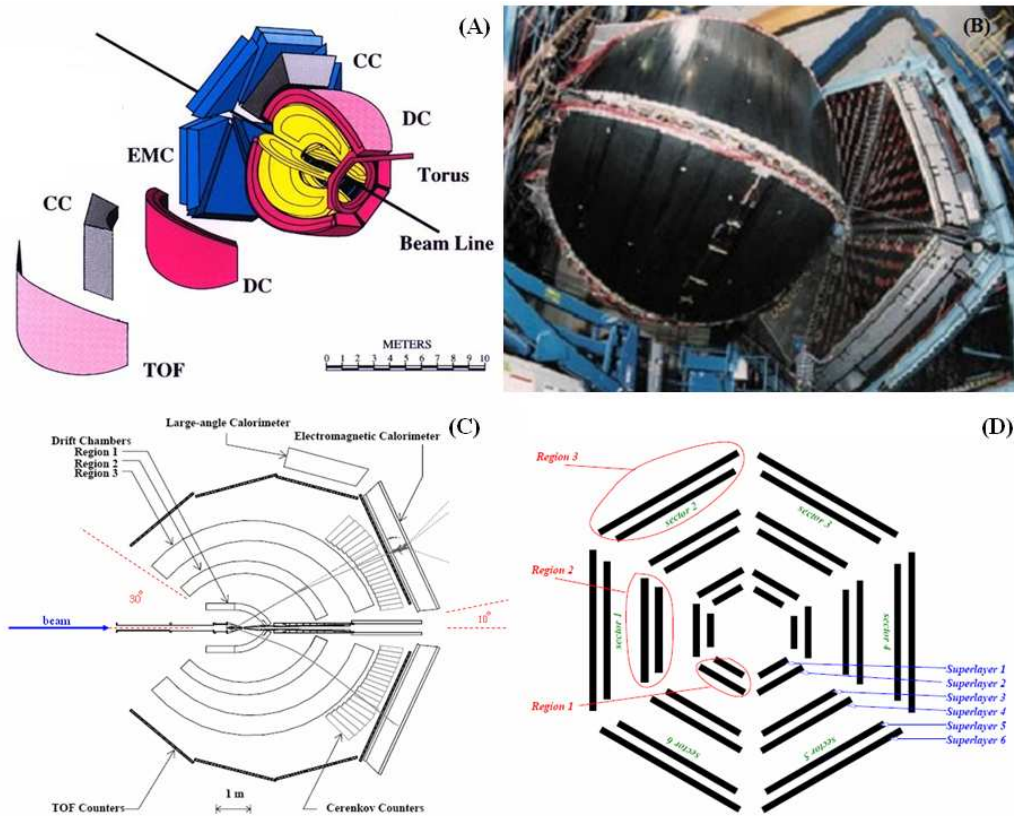


Figure 2: JLAB CLAS detector. The (A) part is a schematic picture of CLAS, the (B) part shows the region 3 of the drift chamber in CLAS, the (C) part is a schematic top view of CLAS, cut along the beam line. Typical photon, electron, and proton tracks (from top to bottom) from an interaction in the target are superimposed on the figure, and the (D) part is a schematic of the CLAS drift chambers.

Each sector is instrumented with multi-wire drift chambers (DC) [4] to determine charged particle trajectories, scintillation counters (SC or TOF) [5] for the measurement of time-of-flight, gas Čerenkov counters (CC) [6] for electron identification, and an electromagnetic calorimeter (EC or EMC) [7] for electron, photon and neutron energy measurement and detection. Close to the target region, a sub-nanosecond coincidence of the tagging spectrometer with a counter (Start Count) [8] measures the start time of a particle trajectory to better than 25 ps. CLAS is called a nearly- $4\pi$  detector, that is, the sensitive region of each sector covers a range of polar angles from  $10^\circ$  to  $150^\circ$  (the beam line in the plot (C) of Figure 2 represents the z-axis in the spherical coordinate system) and the azimuthal range covers approximately 90% at large angles and 50% at forward angles as the sensitive region of CLAS is limited only by the magnet coils.

The bremsstrahlung tagging technique [9] (see appendix A), which is used by the tagging system at JLAB, can tag photon energies over a range from 20% to 95% of the incident electron energy, and is capable of operation with beam energies up to 6.1 GeV. The FROST experiment uses both a linearly-polarized beam and a circularly-polarized beam. A thin, well oriented diamond radiator is used for production of a linearly-polarized photon beam and circularly-polarized photon beams are produced using a beam of polarized electrons incident on the bremsstrahlung radiator.

The frozen-spin target (FROST) is described in more details in appendix B. Figure 3 shows the pre-cooler of the frozen-spin target [10] used in the CLAS-FROST experiment. The FROST target uses butanol ( $C_4H_9OH$ ) as the target material. The target material is cooled to approximately 0.5 K and dynamically polarized outside the spectrometer using a highly homogeneous magnetic field of about 5.0 T. Once polarized, the target is then cooled to a low temperature of 30 mK enough to preserve the nuclear polarization in a more moderate holding field of about 0.5 T. The target is then moved back into the spectrometer, and data acquisition with the tagged photon beam can commence.

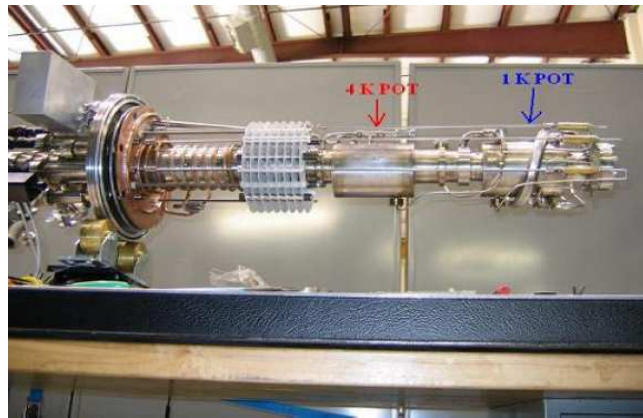


Figure 3: The fully assembled pre-cooler for FROST. Here temperatures of about 1K are reached by evaporating liquid helium. The cylinder that goes through the center of the pre-cooler is a concentric heat exchanger.

### 3.2 The FROST Data

The data for the FROST experiment were taken between November the 3th, 2007 and February the 12th, 2008. The real time to take the data for this experiment is only 72 days and Hall B raw data is acquired in units called runs <sup>3</sup>. In total, runs 603 were accumulated during this period. Run numbers start with 55521 and end with 56233. One run may consist of several files of a fixed size of 2 GB because it would not be convenient to handle one single file with a size of 20 - 60 GB. Figure 4 shows the number of events accumulated during data acquisition.

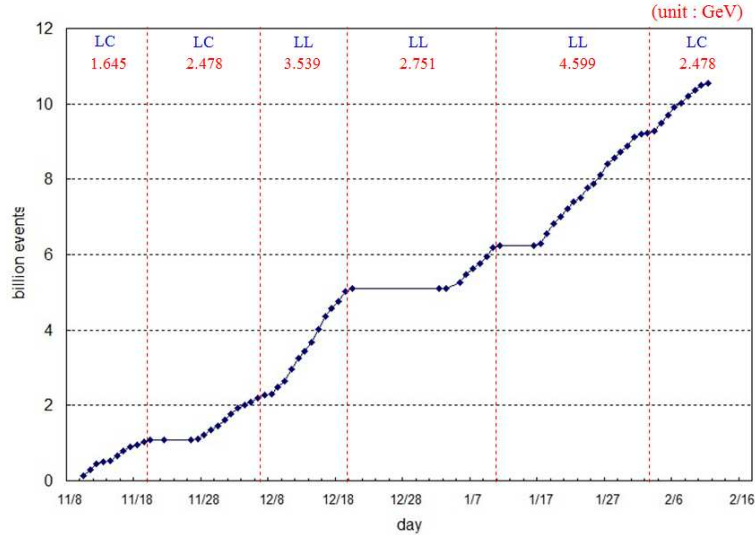


Figure 4: **The number of events for the FROST experiment**

*The FROST experiment uses a variety of electron beam energies. Numbers on the top show electron beam energies in [GeV] used in the FROST experiment. LC means a longitudinal target polarization and a circular beam polarization, and LL means a longitudinal target polarization and a linear beam polarization.*

The possible settings for the beam polarization in the FROST experiment are circular and linear, and for the target polarization, longitudinal and transverse. In the first part of the FROST experiment in which I participated, only longitudinal target polarization was used. If this first part of the FROST experiment, also called g9a <sup>4</sup>, shows promising results on baryon states, a later experiment called g9b will use transverse target polarization. Table 1 summarizes the run list under several conditions such as target polarization, beam polarization, and electron beam energy.

<sup>3</sup>The run in JLAB is used in two concepts. The run in the first concept is a time interval when the data is collected assuming there is no change in the experimental conditions and the run as the second concept is used as the unit of the data accumulated during this time interval. The run means usually the second concept.

<sup>4</sup>the g in the g9a means a gamma ray. The g9a experiment does not use an electron beam but a photon beam

Target Polarization	Beam Polarization	Electron Beam Energy (GeV)	Dates	Run Range
Longitudinal	Circular	1.645	11/10/07 - 11/20/07	55521 - 55595
		2.478	11/27/07 - 12/07/07	55604 - 55676
		2.478	02/04/07 - 02/11/07	56164 - 56233
	Linear	3.539	12/07/07 - 12/20/07	55678 - 55844
		2.751	01/05/08 - 01/11/08	55854 - 55938
		4.599	01/17/08 - 02/03/08	55945 - 56152

Table 1: **The run list of the FROST experiment**

### 3.3 Reconstruction

The information included in the raw data of the FROST experiment consists of QDC (Charge to Digital Converter) and TDC (Time to Digital Converter) channel IDs and values. We need to have some process, called the reconstruction, to convert these data into physical quantities like particle IDs, positions, angles, energies and momenta. This process takes on the order of 15 hours per  $10^6$  events on a mid range Linux PC. The number of events accumulated during the FROST experiment is  $1.05 \times 10^{10}$  events and it would take about 6500 years to reconstruct all raw data using just one linux PC. The data for the FROST experiment is too huge to be managed on one personal computer. The Jefferson Laboratory (JLAB) has a computer system, called the batch farm, which consists of 175 dual CPU computers and is connected to the 100 megabit Ethernet. At JLAB, cooking [12] refers to running some CLAS analysis code on many raw data files by sending them to a farm of computers. Each experiment chooses a chef who manages the process of the cooking. I am serving as the chef in the FROST experiment. The process of reconstructing the raw data requires careful maintaining and good organization skills. In general, the cooking process has three major roles in the reconstruction. First of all, this process assigns each run to an individual farm node. Then, the cooking takes care of files made in any pre or post process. Finally, it attempts to transfer the digital information into physical information. Currently there are 4 main scripts used for the cooking process in the FROST experiment:

- *set\_cook\_env* : A file sourced during login to set up the environment.
- *cook.sh* : A script to do the cooking interactively, or on the farm.
- *create\_jobs.sh* : A script to create jobs to run cooking script on the farm.
- *submit\_jobs.sh* : A script to submit jobs to the farm.

#### 3.3.1 The cooking script (*cook.sh*)

The cooking script reconstructs the raw data with *user\_ana*, which is the FORTRAN-based reconstruction software of the CLAS spectrometer. The *user\_ana* program is configured via a tcl file, *cook.tcl*, which sets



```

Description:
Script to cook a single file locally, or multiple silo files on the farm

Local Use:

cook.sh -l [-t <tclfile>] [-n <events>] <filename> <output_dir>

Options:
-l                It's a local job: cooking is done locally, not on farm
                  and cooks <filename> into <output_dir>, both of which must be specified

-t <tclfile>      Use an alternative to the default (cook.tcl)
-n <events>       Only run user_ana on <events> rather than all.

Farm jobs:

cook.sh -s [-t tclfile] [-s] [-W] [-N]

-s                Silo / Farm job: Files are copied to farm node by LSF.
                  normally cook.sh would be called from within a farm script
                  generated by a tool like create_jobs.sh

-t <tclfile>      Use an alternative to the default (cook.tcl)
-n <events>       Only run user_ana on <events> rather than all.
-W               The output files are copied to work disks.
-S               The output files are copied to SILO
                  NOTE: must have -W or -S or both otherwise data doesn't leave farm!
-d <subdir>      Files copied to work go into passX/versionY/<subdir>

```

Figure 5: The usage of the script, *cook.sh*

up the name of an input and an output file, and switches on or off the required parameters which manage the process of cooking. The FROST data is saved in the BOS format [11] after taking the data. The tcl file determines which of these BOS Banks <sup>5</sup> are written to the output file, and whether or not any data reconstructed is updated in the database for each run analysed. Figure 5 describes how to use the script, *cook.sh*. The cooking script can be run interactively from the command line in the -l mode, that is, in the interactive mode. The -s mode leads the process of the cooking to a farm job.

### 3.3.2 The job creation script (*create\_jobs.sh*)

The job creation script makes job files for the submission to the farm directly or via the script, *submit\_jobs.sh*. Figure 6 gives an account of how to use the *create\_jobs.sh* script. Each run has several files of 2 GB size. This script will manage the number of files, submitted to the batch farm (in the -A option). It selects the personal cooking script made by the user (in the -c option). Also this script defines a range of run numbers and designates the job directory which has all files needed for the cooking.

### 3.3.3 The output files

There are 17,676 BOS files in the raw data of the FROST experiment. Since each file is about 2 GB in size, the FROST experiment accumulated a total of about 35 terabyte of data. Each BOS file name has the usual format *clas\_\*\*\*\*\*.A○○* where the first number represents the run number and the second number its extension. The original BOS files are processed into several output files via the process of reconstruction. The BOS output with

<sup>5</sup>The BOS format is designed as a bank structure.

```

Description: A shell script to create Auger jobs submission scripts for cooking runs

Usage: create_jobs.sh prompt
Asks for input parameters interactively

Usage: create_jobs.sh [opts] <job_dir> <first_run> [<last_run>]

Options:
-A <A numbers>      eg. 'A00 A10 A20' (defaults = all)
-r <runs_per_job>   no of runs in each farm script (defaults = 5)
-c <cook_script>    cook script (defaults = cook.sh)
-o <cook_options>   options passed to cook script eg '-s -W -t mytcl.tcl' (default is '-s -W')
-d <disk_space>    required disk space on farm node in GB (default = 12)
-f                freeze - copies binaries, libs and tars $CLAS_PACK to the job directory
-m                specify alternative email for output (default = clasg13@jlab.org).
-e                mail filtering of farm messages into sensible subdirectories of mail.
-q                only works if mail is coming to the account you're running this script on.
-s                quiet - don't prompt the user for any feedback
-S                submit - go ahead and submit all the jobs to the farm (A DANGEROUS OPTION!)

Job files based on the current pass and version environment will be created (and possibly submitted)
The jobs go into jobs/${RUN}/${COOK_LEVEL}/${COOK_VERSION}/job_dir

For example, with the current environment:

create_jobs.sh -A 'A01 A02' -d 12 -f -m klttest 56660 56690

Creates a directory jobs/g13/pass0/v7/klttest
with jobfiles runs56660-56664.sub, runs56665-56669.sub, ...
requesting 12GB of disk space on farm nodes.
and freezes the current binaries and libraries for these jobs
and sets up mail filtering to relevant Mail subdirectories

```

Figure 6: The usage of the script, *create\_jobs.sh*

the reconstructed events is more than 3 GB in size, thus it is split in two or three files. They are expressed in the usual format, *cooked\_\*\*\*\*\*.A○○.B★★* where the third number represents the number of split runs. The ana-histogram files contain many histograms representing the conditions of each run. A ROOT<sup>6</sup> file is made from the BOS file for the user of the ROOT program. This reconstruction process makes log files which have the information of the process of the cooking and any error that happened during the cooking. Each output file has a different file size and the directory saved. Table 2 is an example of name, file size, and directory of output files when input file is *clas\_055521.A10*.

Description	Nomenclature	Size	Directory
Input File	<i>clas_055521.A10</i>	2 GB	Silo tape
Bos Output	<i>cooked_055521.A10.B00</i>	2 GB	BOS
	<i>cooked_055521.A10.B01</i>	2 GB	
	<i>cooked_055521.A10.B02</i>	51 MB	
Ana-Hist Files	<i>anahist_055521_A10.hbook</i>	11 MB	AnaHistFiles
Log File	<i>run_055521_A10.err</i>	11 KB	LOGS
	<i>run_055521_A10.log</i>	8 KB	
	<i>run_055521_A10.out</i>	55 KB	
Root File	<i>DST_055521.A10.B00.root</i>	408 MB	ROOT
	<i>DST_055521.A10.B01.root</i>	408 MB	
	<i>DST_055521.A10.B02.root</i>	11 MB	

Table 2: Output files name, size and directory with the reconstructed event

<sup>6</sup>ROOT is a program for data analysis developed at CERN

### 3.4 Calibration

In the process of the data acquisition, once a trigger was detected, time counters in detectors start measuring the time until a signal is detected and then they stop and record the data. A general feature of all calibrations is the need to align their timing with the beam radio frequency (RF) <sup>7</sup> time. The TOF scintillator is to measure the time-of-flight of particles mainly and the start-counter detector with the beam RF signal provides the second time reference. The E-counters of the CLAS tagging system check the energy of the photon emitted into the target. The T-counter synchronizes both the time <sup>8</sup> reconstructed in the tagger at the target center and the RF time identified nearest beam bucket at the target center. The start counter, the time-of-flight counter, and the electromagnetic calorimeter in CLAS detector have their timing. Their vertex times <sup>9</sup> are synchronized against the RF vertex time. The timing of the CLAS is aligned together. Table 3 shows the goal of each part of the CLAS detector in the calibration.

Device	Purpose
Tagger	Align T-counter and E-counter timing against the RF beam signal.
Time-of-flight (TOF) Scintillators	Optimize the time and hit position reconstruction, align the 57 paddle timing with each other and within the CLAS detection timing scheme.
Drift Chambers (DC)	Optimize charged tracks reconstruction.
Electromagnetic Calorimeter (EC)	Optimize the time and energy reconstruction.
Start-Counter (ST) Calibration	Align the ST paddles reconstructed within the CLAS detection timing.

Table 3: The purpose of each calibration

Calibration programs generally read in raw or reconstructed data files in BOS format and produce some calibration constants typically in ASCII text format. Calibration is an iterative process. When the calibration of one component is improved, it allows further improvement of other components. For example, if a TOF scintillator measures the time-of-flight of particles more exactly, the EC time will be calibrated more accurately. The CLAS detector can be divided roughly into five parts: tagger, start counter (ST), drift chambers (DC), time-of-flight counter (TOF), and electromagnetic calorimeter (EC). Each part of the CLAS detector has a calibration team according to table 4. Each part of the calibration has a prerequisite stage, that is, the calibration of certain detector components can only start after other calibrations are finalized. The order of the calibration in the FROST experiment is Tagger - TOF and ST - DC and EC.

<sup>7</sup>The accelerator in JLAB makes an electron beam of which the period is 2.004 nanoseconds, called the machine RF time, that is, an electron beam bucket is supplied to the target about every 2 nanoseconds.

<sup>8</sup>The location of T-counter is shown in Figure 11. T-counter measures the travel time of the electron from the T-counter to the radiator and then recalculates the travel time of the photon beam from the radiator to the target center. The photon beam which is corresponded to the electron passed T-counter, is identified. We compare the time calculated at the tagger with the machine RF time in the same distance from the radiator to the target center. The photon beam, which makes the event in the CLAS spectrometer, is identified.

<sup>9</sup>The TOF vertex time is the vertex time of the photon beam calculated from TOF scintillator to the target inversely. Other vertex times have the same concept.

Item	Contact	Prerequisite
Cooking	Sungkyun Park (FSU)	all calibrated
Tagger Calibration	Liam Casey (CUA), Franz Klein (CUA)	none
TOF Calibration	Robert Coyne (UMASS), Hideko Iwamoto (GWU), Arthur Sabintsev (GWU)	TAG
ST Calibration	Mukesh Saini (FSU)	TAG
DC Calibration	Sean Kuvin (FSU), Evan McClellan (FSU), Sungkyun Park (FSU), Volker crede (FSU)	TOF
EC Calibration	Simona Malace (USC)	TOF
Beam Polarization (Circ.)		none
Beam Polarixation (Lin.)	Stuart Fegan (U of Glasgow)	none
Target Polarization	Jo McAndrew (U of Edinburgh)	none
DC Alignment	Sungkyun Park (FSU)	DC
Momentum corrections		all cooked
Energy loss corrections	Jo McAndrew (U of Edinburgh)	none
Bookkeeping	Hideko Iwamoto (GWU)	all cooked

Table 4: The man power list of Cooking and Calibration in the g9a experiment

The FSU group in the g9a experiment takes the responsibility for cooking, ST calibration, and DC calibration [13] in the part of the cooking and calibration. I have committed to parts of the cooking and DC calibration in the FROST experiment. In general, a set of representative runs dispersed evenly throughout the beamtime is selected for calibration. These runs are calibrated and cooked over several iterations until all subsystems are considered to be satisfactorily calibrated. And then the calibrations are applied to the whole run period, and a bigger subset of the whole data set is cooked to check the quality and consistency of the calibrations. Typically, at this stage, 2 files per run would be cooked, resumming 5-10% of the total run statistics.

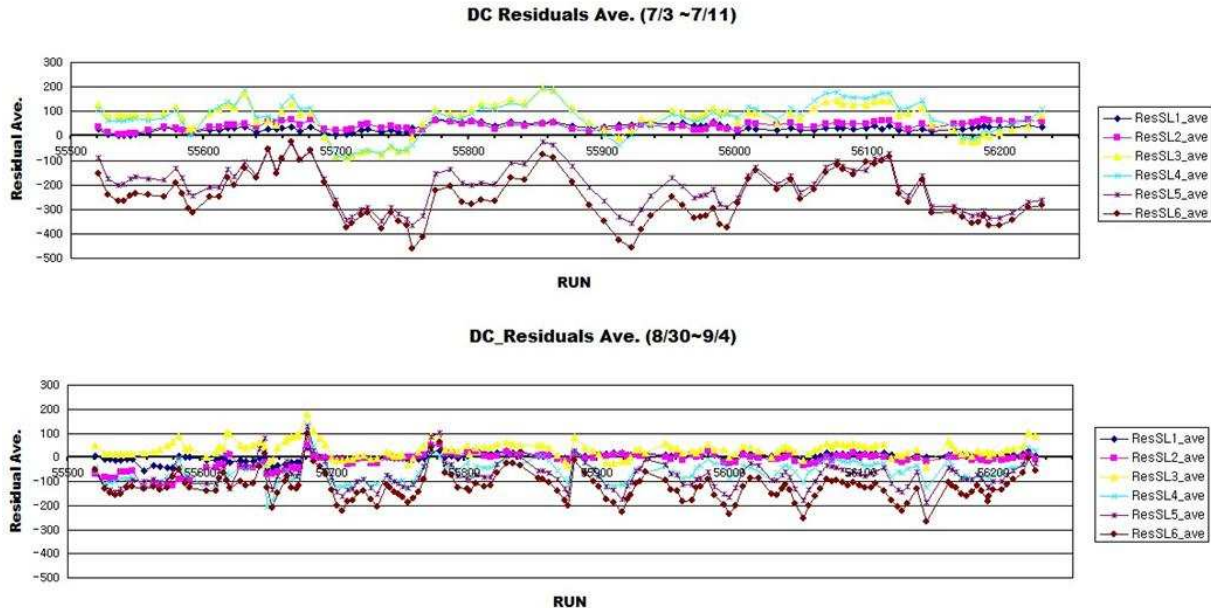


Figure 7: plots of DC Residual Ave.

The two plots of Figure 7 are made to check the status of the DC Calibration. The drift chamber is set up to determine the particles' tracks in the CLAS detector. In Figure 7, the top plot was made before the first iteration of DC calibration and the bottom plot is based on the data made after the second iteration of DC calibration. We can confirm that the values of the residuals (see appendix C for more details) in every superlayer as shown in the plot (D) of Figure 2 are improved, that is, values tend to approach zero when we compare the new ones with the old ones. However, residuals of superlayers 5 and 6 are not stable, but fluctuating and values of residuals are far from zero. These problems need to be improved in the following iterations.

### 3.5 Monitoring

Monitoring programs produce histograms which are based on the offline database. Figure 8 is a screenshot of the monitoring page for the FROST experiment. The user can select the variables which indicate histograms to view on the left side of the web page. Monitoring programs produce three kinds of plots generally. The first plots indicate that the system is working properly. In Figure 8, variables such as beam position, beam sigma, and CPU time for cooking show the basic condition of each run. The second set of plots provides useful information on some basic particle properties and their hit pattern for the concept of physics and this website gives basic information on the proton,  $\pi^+$ ,  $\pi^-$ , and kaon. Finally, the monitoring programs also make plots to check the quality of the existing calibration. The part of the section "DC Residuals" of Figure 8 has plots to check the status of the DC calibration.

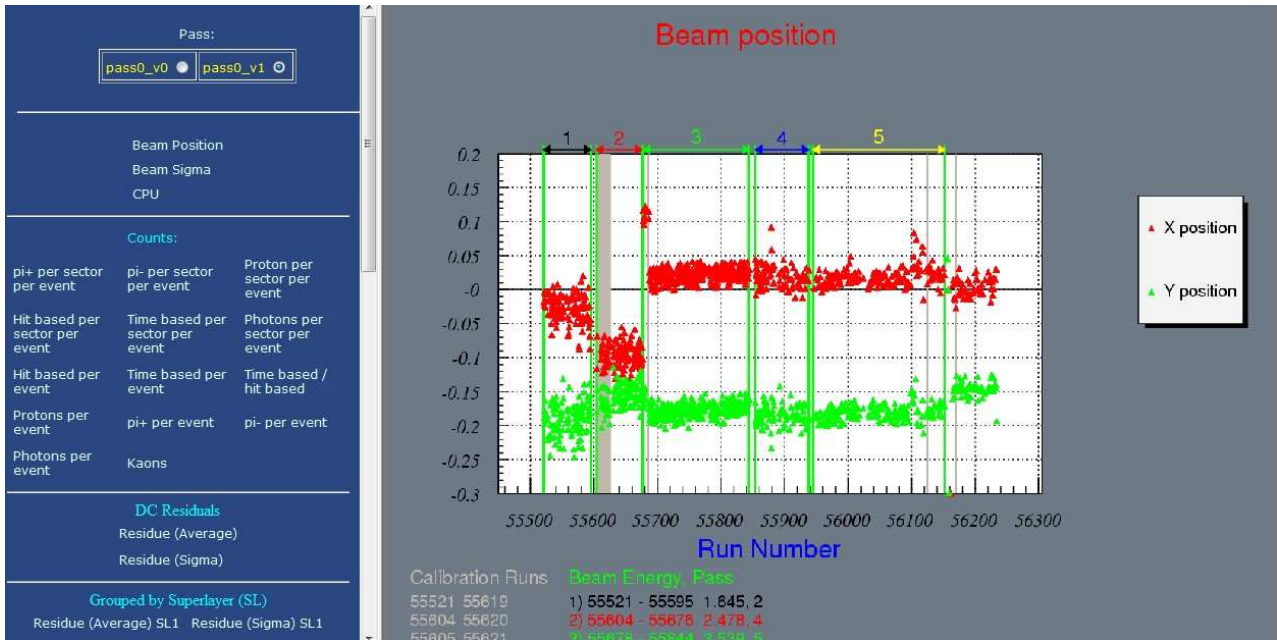


Figure 8: The monitoring page for the g9a online mysql variables.

The user can select the pass <sup>10</sup> with the buttons at the top of the page. In the Figure 8, pass0\_v1 means that pass is 0 and version is 1. The pass and version is decided for the process of calibration. The cooking level is decided as a pass number. The pass 0 is defined as the beginning stage of the calibration. In this pass, calibrations are usually bad. What needs to be improved for calibration is searched and another version of pass 0 is selected. In pass 0, a few percent of the data is used for the calibration. Once the condition of calibration is good, pass is changed from 0 to 1. In pass 1, all the files of the data are used for calibration. I make the monitoring program for the FROST experiment with reference to the one of another experiment group. I update these monitoring pages after changing the version. I maintain this monitoring pages until now.

## 4 The concept of physics for my dissertation

Polarization observables are very useful to disentangle broadly overlapping states of resonances, especially at higher masses. As polarization observables are sensitive to those small resonant contributions, those parameters will contribute to evaluate  $N^*$  parameters. Figure 9 shows decay angles in a 3-particle final state. The  $\pi^-\pi^+$  final state requires 5 independent invariables, for example,  $\phi$ ,  $\theta$ ,  $k$ ,  $m_{p\pi^+}$ , and  $m_{\pi^+\pi^-}$ .

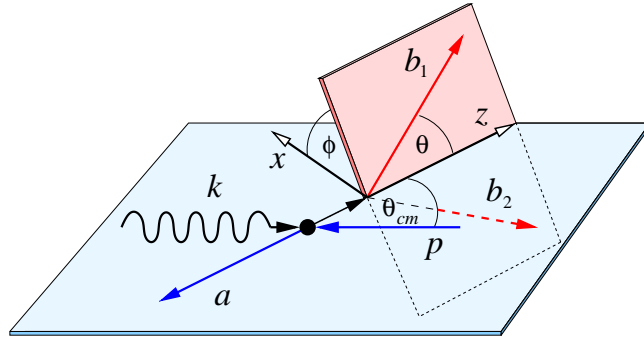


Figure 9: **Decay angles in a 3-particle final state:**  $\phi$  indicates the angle between the production plane and the plane formed by two of the final-state particles

For  $\gamma p \rightarrow p\pi^+\pi^-$  without measuring the polarization of the recoiling nucleon, the differential cross section is given by [14]

$$\begin{aligned} \frac{d\sigma}{d\Omega} = & \sigma_0 \{ (1 + \vec{\Lambda}_i \cdot \vec{\mathbf{P}}) \\ & + \delta_{\odot} (\mathbf{I}^{\odot} + \vec{\Lambda}_i \cdot \vec{\mathbf{P}}^{\odot}) \\ & + \delta_l [\sin 2\beta (\mathbf{I}^{\mathbf{s}} + \vec{\Lambda}_i \cdot \vec{\mathbf{P}}^{\mathbf{s}}) \\ & \cos 2\beta (\mathbf{I}^{\mathbf{c}} + \vec{\Lambda}_i \cdot \vec{\mathbf{P}}^{\mathbf{c}})] \} , \end{aligned} \quad (1)$$

<sup>10</sup>The pass means the iteration of the cooking .

where  $\vec{\mathbf{P}}$  represents the polarization asymmetry that arises if the target nucleon is polarized and  $\vec{\Lambda}_i$  indicates the polarization of the initial nucleon. The degree of circular polarization in the photon beam is denoted by  $\delta_{\odot}$ , the degree of linear polarization is denoted by  $\delta_l$ , and  $\beta$  denotes the angle between the direction of polarization and the  $x$ -axis. The  $\mathbf{I}^s$  and  $\mathbf{I}^c$  are the sine and cosine contributions of the observables arising from the use of a polarized photon beam. The photon polarization asymmetry  $\mathbf{I}^{\odot}$  has already been measured at Jefferson Laboratory [15] for  $\gamma p \rightarrow p\pi^+\pi^-$  and uniquely.

To measure Polarization Observables, the following combinations of beam and target polarization will be used:

- **Linearly-polarized beam on a transversely-polarized target** - Measurement of  $\mathbf{P}_x^{s,c}, \mathbf{P}_y^{s,c}$
- **Circularly-polarized beam on a transversely-polarized target** - Measurement of  $\mathbf{P}_x^{\odot}, \mathbf{P}_y^{\odot}$
- **Linearly-polarized beam on a longitudinally-polarized target** - Measurement of  $\mathbf{P}_z^{s,c}$
- **Circularly-polarized beam on a longitudinally-polarized target** - Measurement of  $\mathbf{P}_z^{\odot}$

The g9a experiment uses only a longitudinally-polarized target so observables to be found in this experiment are  $\mathbf{P}_z^s, \mathbf{P}_z^c$ , and  $\mathbf{P}_z^{\odot}$ . The main goal for my dissertation is to measure  $\mathbf{P}_z^{\odot}$ . Now Equation 1 has twenty kinds of observations and needs to be simplified to focus on a few observations. Equation 1, in the case of a circularly-polarized beam on a longitudinally-polarized target, can be written as:

$$\frac{d\sigma}{dx_i} = \sigma_0 \{ (1 + \Lambda_z \cdot \mathbf{P}_z) + \delta_{\odot} (\mathbf{I}^{\odot} + \Lambda_z \cdot \mathbf{P}_z^{\odot}) \}. \quad (2)$$

In the following,  $\rightarrow$  and  $\leftarrow$  indicate circular polarization of the beam in its two possible setting while  $\Rightarrow$  and  $\Leftarrow$  indicate longitudinal target polarization paralleled and anti-paralleled to the beam. Flipping the polarization of the beam makes the number of observables of Equation 2 reduced.

$$(\rightarrow\Rightarrow - \leftarrow\Rightarrow) := \frac{d\sigma(\rightarrow\Rightarrow)}{dx_i} - \frac{d\sigma(\leftarrow\Rightarrow)}{dx_i} = 2 \cdot \sigma_0 \{ \delta_{\odot} (\mathbf{I}^{\odot} + \Lambda_z \cdot \mathbf{P}_z^{\odot}) \} \quad (3)$$

$$(\leftarrow\Leftarrow - \rightarrow\Leftarrow) := \frac{d\sigma(\leftarrow\Leftarrow)}{dx_i} - \frac{d\sigma(\rightarrow\Leftarrow)}{dx_i} = 2 \cdot \sigma_0 \{ \delta_{\odot} (-\mathbf{I}^{\odot} + \Lambda_z \cdot \mathbf{P}_z^{\odot}) \} \quad (4)$$

The single polarization observables  $\mathbf{I}^{\odot}$  does not depend on the target polarization and occurs if only the beam is circularly polarized. To measure  $P_z^{\odot}$ , it is necessary to flip the beam and the target polarization together.

$$(\rightarrow\Rightarrow - \leftarrow\Rightarrow) + (\leftarrow\Leftarrow - \rightarrow\Leftarrow) := \frac{d\sigma_{3/2}}{dx_i} - \frac{d\sigma_{1/2}}{dx_i} = 4 \cdot \sigma_0 \cdot \delta_{\odot} \cdot (\Lambda_z \cdot \mathbf{P}_z^{\odot}). \quad (5)$$



The sample analysis shown in Figure 10 is done to check the status of the current calibration. The mass of the neutron state, known already, is recalculated via the FROST data.

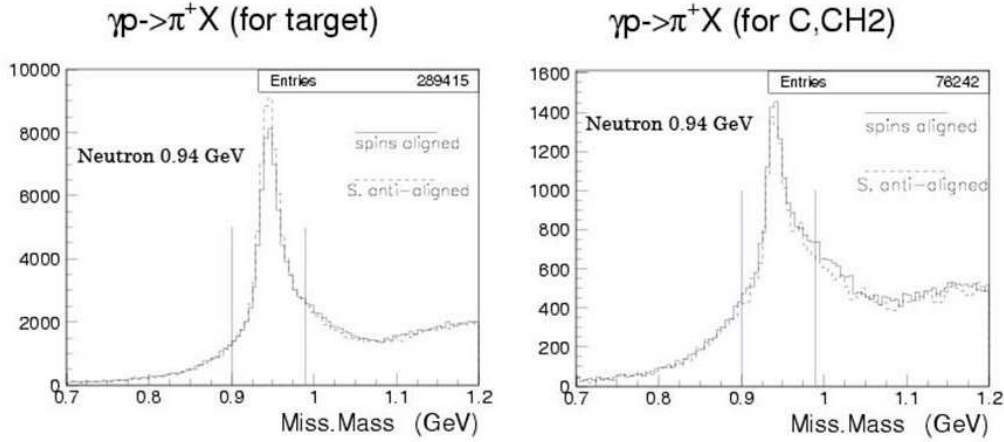


Figure 10: Searching the missing mass in sample analysis  $\gamma p \rightarrow \pi^+ n$ . The left plot is made from the polarized target and the right plot from the unpolarized target.

## A The tagging system in JLAB

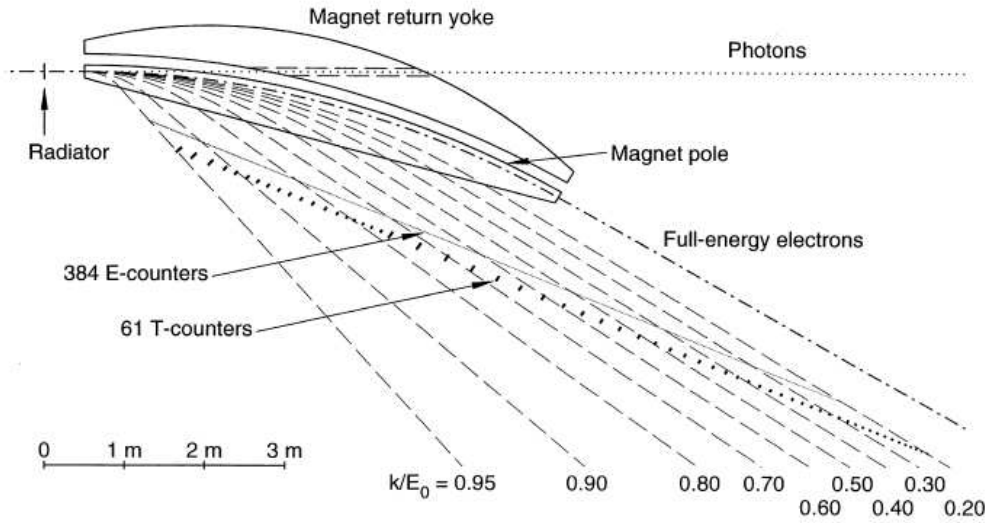


Figure 11: Overall geometry of tagging system in JLAB. Important details referenced in the text include the shape of the magnet pole, the straight-ahead photon path through the magnet yoke, and the relative locations of the hodoscope E- and T-planes.

The tagging system [9] in JLAB is the photon tagger in the multi- GeV energy range to combine high resolution ( $\sim 10^{-3} E_0$ ) with a broad tagging range (20% - 95% of  $E_0$ ). A single dipole magnet as shown in Figure 11 is combined with a hodoscope containing two planar arrays of plastic scintillators to detect energy-degraded



electrons from a thin bremsstrahlung radiator. The first layer of 384 partially overlapping small scintillators provides photon energy resolution, while the second layer of 61 larger scintillators provides the timing resolution necessary to form a coincidence with the corresponding nuclear interaction triggered by the tagged photon. Electrons from the CEBAF accelerator strike a thin target (the “radiator”) just upstream from the magnetic spectrometer. The system is based upon the electron bremsstrahlung reaction in which an electron of incident energy  $E_0$  is decelerated (scattered) by the electromagnetic field of a nucleus, and in the process emits an energetic photon (gamma ray). The energy transferred to the nucleus is negligibly small, so the reaction obeys the energy conservation relation

$$E_\gamma = E_0 - E_e$$

where  $E_e$  is the energy of the outgoing electron and  $E_\gamma$  is the energy of the emitted photon. Since  $E_0$  is uniquely determined by the accelerator, a measurement of the outgoing electron energy by a magnetic spectrometer thus provides a determination of the photon energy.

## B Frozen-Spin Target (FROST) and Magnets

The FROST target uses butanol ( $C_4H_9OH$ ) (Table 5) as the target material for both longitudinal and transverse polarization with a minimum amount of material between the target and CLAS. The FROST target operates in a position such that the target cell is in the geometrical center of CLAS. The target cooling system is a horizontal piece, 200 cm in length with a maximum diameter of 25 cm. Since the material between the target and the detectors needs to be minimal, the target is polarized outside of CLAS and then, during data-taking, resides in a low magnetic holding field.

Chemical structure	$C_4H_9OH$
Dilution factor	10/74
Length	50 mm
Diameter	15 mm
Density	0.985 g/cm <sup>3</sup>
Packing factor	0.62 ± 0.04
Effective density	0.611 g/cm <sup>3</sup>
Longitudinal polarization (average)	0.80
Transverse polarization (average)	0.80

Table 5: **Target properties for the Frozen-Spin Butanol Target**

The polarizing magnet dynamically polarizes the target material through microwave irradiation in a strong magnetic field of 5 T in an environment of 0.5 K. In the process of dynamic polarization, free electrons are

polarized by a strong magnetic field and then microwaves are used to transfer that polarization to the nucleon. After the target has attained the maximum degree of polarization, the dilution refrigerator and holding magnet is turned on. This freezes the spin of the protons and preserves it in a 0.5 T magnetic field at a temperature of 50 mK. The target is then moved into position in the center of CLAS. A butanol target with an initial proton polarization of 90% has a relaxation time of several days under this procedure giving sufficient time for a useful polarized target experiment. Once the target's polarization has declined down to about 50~60%, the target is then taken out of CLAS, put back into the high magnetic field and repolarized. The target cell itself is 50 mm in length and 15 mm in diameter. The target material is butanol ( $C_4H_9OH$ ) with a dilution factor (fraction of polarizable nucleons) of approximately 13.5%. A similar target has been constructed and used at the German photonuclear facilities such as Mainz and Bonn with maximum polarizations of 85% to 95%.

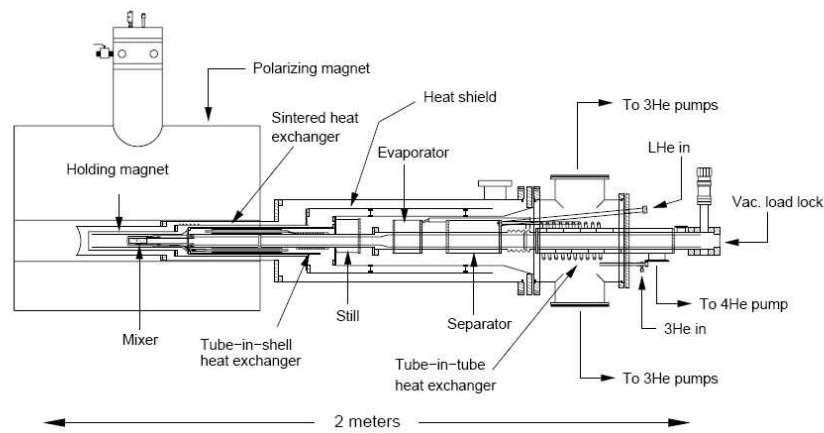


Figure 12: Schematic drawing of the CLAS Frozen Spin Target located inside the 5 T polarizing magnet.

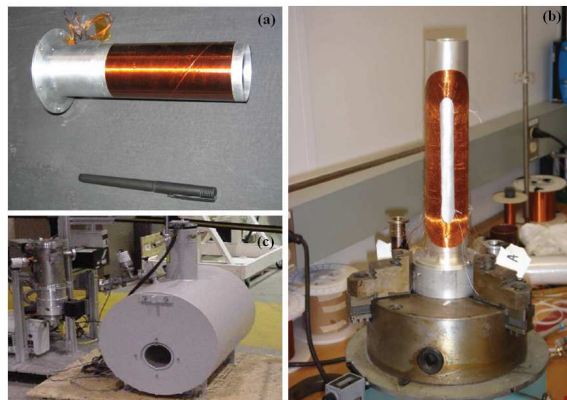


Figure 13: The (a) plot is the longitudinal holding magnet, the (b) plot is the transverse holding magnet, and the (c) plot is the polarizing magnet.

The polarizing magnet used with the FROST target is a horizontal superconducting solenoid magnet capable of producing a field of 5 T with a hole 130 mm in diameter bored through it as shown in the (c) plot of Figure 13. The current design of the holding magnet (both the longitudinal as shown in the (a) plot of Figure 13 and transverse holding magnet as shown in the (b) plot of Figure 13 ) produces a field of 0.5 T with a homogeneity of better than 1% within the target cell volume.

## C Drift chamber calibration

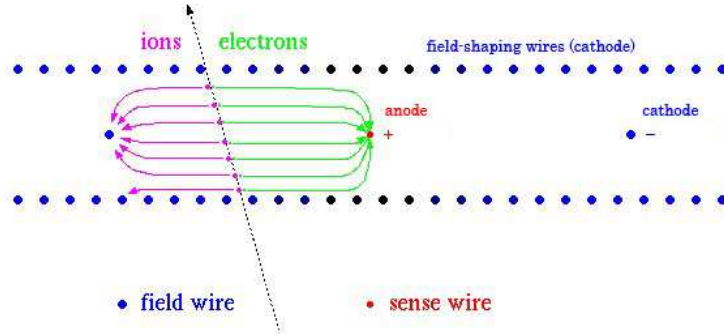


Figure 14: **Typical arrangement of electrodes for drift chamber cell.**

Drift chambers (DC) are in a magnetic field and from the curvature we can determine the momentum of particle. DC are used to measure where a charged particle has crossed a virtual plane. For this purpose thin wires are fixed in a volume filled with a special gas (CLAS uses 90% argon - 10%  $CO_2$  gas mixture as a gas system) in a way, that the wires form cells shown in Figure 14. The DC of CLAS uses a quasi-hexagonal pattern with six field wires surrounding one sense wire shown in Figure 15 as the cell form. Inside these cells a traversing charged particle ionizes the gas. Due to the electrical potentials applied to the field-shaping wires the electrons drift to the sense wire and the connected electronics measure this current.

The drift time refers to the time it takes electrons to drift to the nearest sense wire from the place where the high-energy particle ionized an atom shown in Figure 15. Any three sense wires are only nearby in one place so a set of “hits” on these three fixes a particle track in this region. By measuring the drift time shown in the (b) plot of Figure 16, the location of the original track can be determined much more precisely than the actual spacing between the wires. This distance of closest approach of the charged particle to the sense wire is called DOCA in CLAS.

Figure 16 shows histograms needed for DC calibration. The left plot of figure 17 is a histogram made in the process of DC calibration and describes the relation between fitted DOCA and the drift times. The fitted DOCA are obtained from fits to global tracks (i.e. fits which include all layers). That is to say, the trajectory in

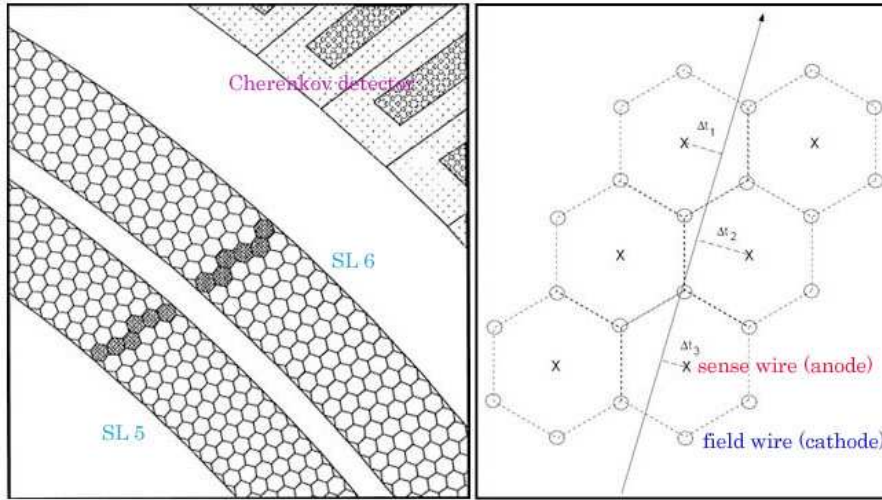


Figure 15: The left plot represents portion of an Region 3 sector showing the layout of its two superlayers. The sense wires are at the center of each hexagon and the field wires are at the vertices. A passing charged particle is shown by the highlighted drift cells that have fired. The right plot represents schematic diagram showing a charged particle track. The individual hexagonal drift cells are identified by the dashed line around the perimeter of each.  $\Delta t_i$  represents the drift time measured in each drift cell.

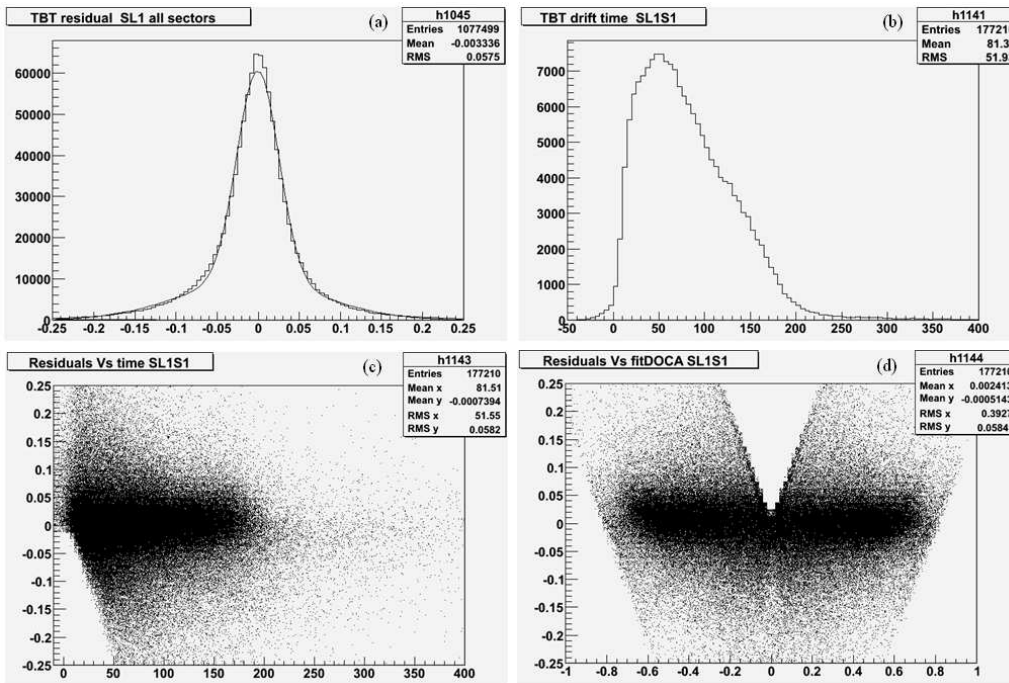


Figure 16: Histograms needed for DC calibration. The (a) histogram represents the residual average of the time-based tracking (TBT) in superlayer 1 and all sectors, the (b) histogram describes the drift time of TBT measured in superlayer 1 and sector 1, the (c) histogram shows the relation of residuals versus the drift time in superlayer 1 and sector 1, and the (d) histogram shows the relation of residuals and fitted DOCA in superlayer 1 and sector 1.

drift chamber can be rebuild in a first stage without information from other detectors in a hit-based (HB) track. This trajectory data is fitted DOCA. The program for DC calibration calculates the drift velocity function for every superlayer in every sector fitting shown in the right plot of Figure 17. This program takes out calculated DOCA from the relation of the drift velocity function and the drift time. The residual is defined as the difference between calculated DOCA and fitted DOCA. Going from the rough HB track to a complete time-based (TB) track, requires timing alignment of the time-of-flight measurement. The goal in DC Calibration is that the value of the residual in each superlayer become around zero.

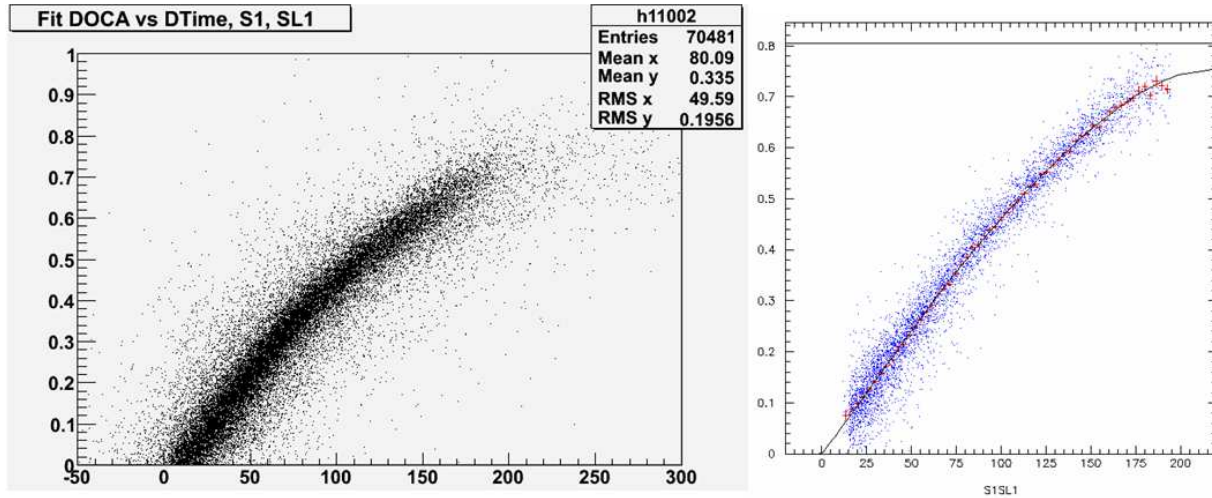


Figure 17: Fit DOCA vs Dtime S1SL1

## References

- [1] S. Capstick and N. Isgur, “Baryons in a Relativized Quark Model with Chromodynamics”, *Phys. Rev.* **D34**, 2809 (1986)
- [2] L. Glozman and D. Riska, “The Spectrum of the nucleons and the strange hyperons and chiral dynamics”, *Phys. Rept.* **268**, 263 (1996), hep-ph/9505422
- [3] U. Loring, K. Kretzschmar, B. Metsch, and H. Petry, “Relativistic quark models of baryons with instantaneous forces”, *Eur. Phys. J.* **A10**, 309(2001), hep-ph/0103287.
- [4] D.S. Carman *et al.* *Nucl. Instr. and Meth. A* **449**, (2000) 81.
- [5] E.S. Smith *et al.* *Nucl. Instr. and Meth. A* **432**, (1999) 265.
- [6] P. Stoler *et al.* *Nucl. Instr. and Meth. A* **465**, (2001) 414.

- [7] L.C. Smith *et al.* Nucl. Instr. and Meth. A **460**, (2001) 239.
- [8] G.S. Mutchler *et al.* Nucl. Instr. and Meth. A **556**, (2006) 246.
- [9] D.I. Sober *et al.* Nucl. Instr. and Meth. A **440**, (2000) 263.
- [10] C. D. Keith and O. Dzyubak, “DESIGN OF A FROZEN SPIN TARGET FOR CLAS”, ckeithGDH2004.
- [11] D. Cords *et al.*, “CLAS Event Format with BOS”, CLAS-NOTE 94-012.
- [12] L. Todor, “G1C Data Calibration and Cooking Procedures, characteristics, information”, CLAS-NOTE 2002-017.
- [13] D. Lawrence, M. Mestayer, “CLAS Drift Chamber Calibration: Software and Procedures”, CLAS-NOTE 1999-018
- [14] W. Roberts and T. Oed, “Polarization Observables for Two-Pion Production off the Nucleon”, (2004), nucl-th/0410012.
- [15] S. Strauch *et al.*, [CLAS Collaboration], “Beam-Helicity Asymmetries in Doubly-Charged-Pion Photoproduction on the Proton”, Phys. Rev. Lett. **95**, 162003 (2005).